International Journal of Advances in Computer Science & Its Applications – IJCSIA
Volume 4: Issue 4 [ISSN 2250-3765]
Publication Date : 27 December,2014

Deflection of Wide Hidden Beams in One-Way Slab Systems: A Nonlinear Finite Element Study

Ziad N. Taqieddin

***Abstract*—The effectiveness of compression reinforcement in controlling the deflection of a wide-hidden continuous reinforced concrete beam is studied using nonlinear finite element (FE) simulations. Concrete Damaged-Plasticity and reinforcing steel Elasto-Plasticity are used in the nonlinear FE simulations of ABAQUS. Results are compared to Elastic FE simulations as well as to conventional code procedures.**

***Keywords*—Reinforced Concrete, Nonlinear Modelling, Finite Elements, Deflection Control, Damage Mechanics.**

I. Introduction

Wide-hidden reinforced concrete (RC) beams are frequently used in ribbed and solid one-way slab systems in Jordan. The reduced amount of formwork during construction and the aesthetically appealing view of the continuous slabs are both reasons and advantages of adopting such hidden beams. On the other hand, these shallow beams often exhibit large amounts of deflection unless a considerable percentage of compression steel reinforcement is added as a remedy. In this work, the effectiveness of compression reinforcement in resisting the deflection of a wide-hidden continuous RC beam is studied. The deflection calculations are performed three times: initially according to the American Concrete Institute (ACI) 318M-11 Code [1] procedure, followed by two types of finite element (FE) simulations using ABAQUS [2]. Elastic FE analysis is carried out to produce a lower bound on deflection, while a nonlinear FE analysis is used to obtain a more physically based approximation. The nonlinear FE analysis uses concrete Damaged-Plasticity as well as reinforcing steel Elasto-Plasticity, both being built-in capabilities of ABAQUS.

The depth of hidden beams is dictated by the slab thickness. Ribbed slabs flourish a better host for such beams due to their enlarged depths as compared to solid slabs. Support locations and beam spans are checked to ensure that the depth/span ratios required by the ACI Code are satisfied. Table 9.5(a) in Section 9.5.2.2 of the ACI Code provides general guidelines for these ratios unless more accurate procedures are employed to calculate deflections. The same table states that the depth/span ratios are for "members not supporting or attached to partitions or other construction likely to be damaged by large deflections". When that is not the case, or when the Code's procedure reveal the inadequacy of such hidden beams to meet the deflection requirements, engineers often resort to the addition of compression steel reinforcement in an attempt to drag midspan deflection values back into the Code's permissible range. Studying the effectiveness of compression reinforcement on deflection control is the main objective of this work, and is illustrated by considering the details of a three span continuous hidden beam in an already existing residential building. The structural system consists of ribbed one-way slabs of 31cm depth as shown in Fig. 1. All the materials' specific weights and design loads are obtained from the Jordanian Code of Loads and Forces [3]. The total dead load (D) is calculated using Fig. 1 and is taken as 10.6 kN/m^2 (including hollow concrete block partitions) while the live load (L) on a typical floor is taken as 2 kN/m^2. The hidden beam under consideration is 1m wide and is symmetrically continuous over three spans of 5.345m for exterior spans and 6.2m for the interior span (center to center between supports). The tributary width assign to this beam is 4.587m resulting from two identical slab spans. Supports are 75cm x 30cm columns reinforced with 12 ϕ 20mm distributed on the long faces. Beam longitudinal Reinforcement distribution is shown in Fig. 2, while shear reinforcement consists of four legged 10mm stirrups at any cross section on the beam (@15mm) or columns (@20mm). Throughout this work, a compressive strength of concrete $f_c^{'}$ = 28MPa and a yield strength of reinforcing steel f_y = 420MPa are considered.

Ziad N. Taqieddin / Assistant Professor, Civil Engineering Department
College of Engineering / Applied Science Private University (ASU)
Amman / Jordan

II. Methods of Analysis

The maximum deflection values are calculated using three different methods: initially according to the provisions of Section 9.5 of the ACI Code, followed by two types of finite element simulations; Elastic and Inelastic. These methods are explained in details below.

A. *ACI Provisions for Deflection Control*

The effective moment of inertia procedure for continuous beams is used. The midspan and exterior moments are obtained from structural analysis. These moments are then used to calculate the effective moment of inertia, I_e, for each span according to the averaging procedure described in [4]. The structural analysis is then repeated but this time using the I_e values calculated for each span. Fifty percent of the live load acting on the beam is assumed to be sustained (SL) for a duration of 5 years. The deflection resulting from D, D+SL, D+L, L, SL, and the long term deflection (LT) for each span are summarized in Table 1. Location of the maximum deflection is measured from the left end of each span (local coordinates). The ACI factor $\lambda_\Delta = \xi/(1+50\rho')$ shows the effect of the compression reinforcement on reducing long term

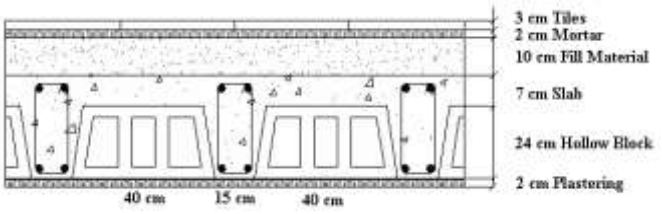

Figure 1. Slab layers/composition

deflection. It is observed from Table 1 that the maximum value of deflection occurs in the exterior span and exceeds the maximum permissible limit of $\ell / 480$ = 11.2mm for floors supporting nonstructural elements likely to be damaged by excessive deflections (ACI Table 9.5(b)). It should be noted here that no live load patterns where considered to maximize the interior span deflection since the governing deflection is located in the exterior span.

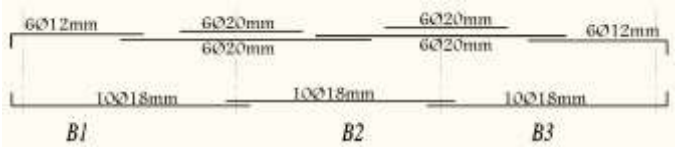

Figure 2. Beam reinforcement distribution

B. *Elastic FE Analysis*

This step is performed to establish a reference for the nonlinear FE analysis. A FE mesh is created in ABAQUS using linear quadrilateral plane stress elements, and is shown in Fig. 3. Taking into account the symmetry of the structure, only an interior column and the surrounding half spans are considered. The flexural and shear reinforcement in the column and half spans are modeled in accordance with the structural plans of the building. The mesh size selected is 1cm, with a total number of elements reaching 22,760. Only 30cm

TABLE I. MAXIMUM DEFLECTION VALUES

	Maximum Deflection (mm)	
Load/Span	***Exterior Span***	***Interior Span***
D	8.6	4.7
D+SL	9.6	5.4
D+L	10.5	6.1
SL	1.0	1.4
L	1.9	0.7
LT	13.2	7.7
Location (m)	2.3	3.1

of the column height above and below the beam are modeled, and boundary conditions simulating the actual scenario (strong column – weak beam) are applied. Linear elastic concrete and steel material properties are assigned to the FE mesh (stated in the next section), and the depth (perpendicular to page) of each element is applied according to the type of material that the finite element represents. The static equivalent transformed section properties are employed. Tributary load on each beam is uniformly distributed over the clear spans (kN/m). The results of this elastic FE simulation are compared to those of the nonlinear FE analysis described in the next section. The direct stress component (S11) of the simulation is shown on the deflected shape in Fig. 4 as a sample of the output file.

C. *Nonlinear FE Analysis*

In the nonlinear FE simulation using ABAQUS, Concrete Damaged Plasticity is assigned to the concrete material while isotropic strain hardening with a very shallow tangent stiffness is assigned to the reinforcing steel material (elastic perfectly plastic steel behavior introduced convergence problems). The elastic properties of both materials remained the same as those of the previous section. A summary of the experimental material parameters for $f_c^{'}$ = 27.6MPa can be found in Lee and Fenves [5], and concrete material tensile and compressive

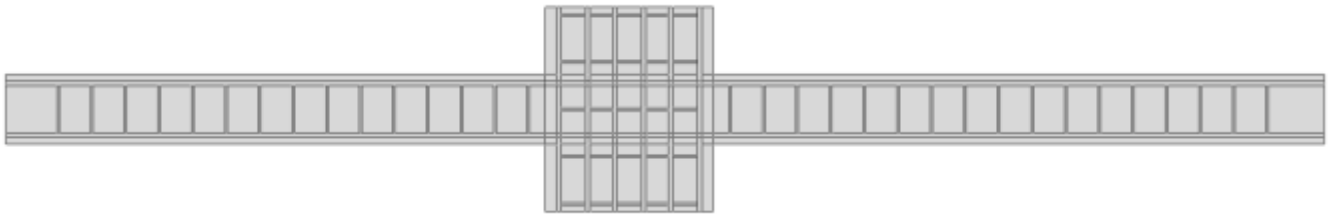

Figure 3. Beam FE representation

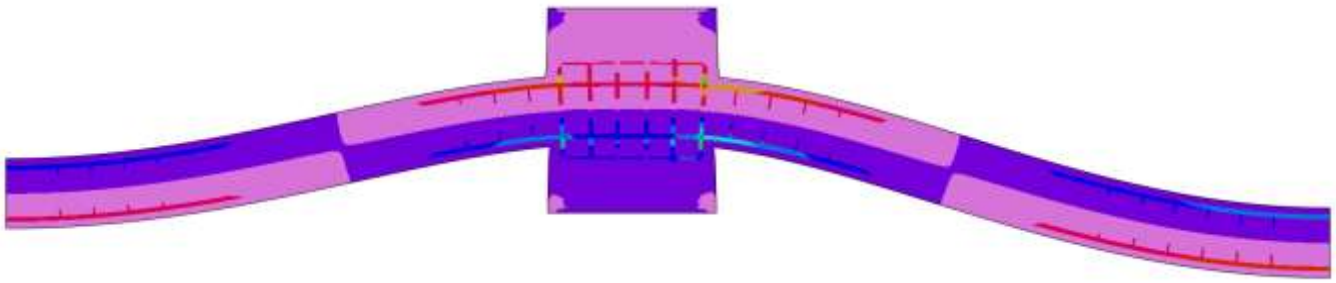

Figure 4. Direct stress contour, S11

damage evolution curves are adapted from Taqieddin et al. [6]. Reinforcing steel material properties are: elastic Young's modulus 200GPa, Poisson's ratio 0.3, and ultimate stress 440MPa at an inelastic strain of 0.005. The stress-strain as well as stress-displacement relations are shown for the elastic and inelastic (EPD) simulations in Fig. 5. It is important here to note that the maximum deflection in both FE simulations (elastic and inelastic) was located at the middle of the interior span, in contrary to the results of structural analysis in Table 1. The deflections in Fig. 5 are for full service loads (D+L) and using the compression steel ($A_s^{'}$) shown in Fig. 2. The FE deflections are smaller than those predicted by the ACI Code procedure, but are by no means less significant.

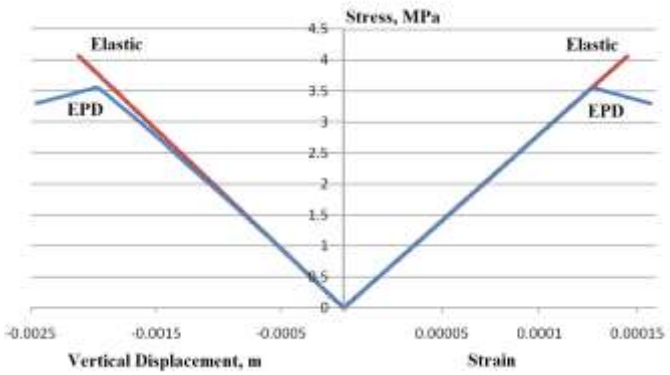

Figure 5. Stress, strain, and deflection at middle of interior span

Fig. 6 shows tensile damage growth in concrete at the middle of the interior span, while Fig. 7 shows the growth of the same parameter in concrete around an interior column, with the same contour colors, and using $A_s^{'}$ shown in Fig 2. An interesting outcome is that concrete at the beam/column conjunction reaches severe computational values of tensile damage under service loads (D+L). Using less compression steel at midspan only makes the situation worse at the support section and eventually leads the FE simulation to diverge and terminate. This is justified by the fact that decreasing the midspan compression reinforcement increases the midspan deflection and imposes huge burdens on concrete at the support section. On the other hand, increasing the compression steel at midspan in order to decrease deflections becomes adversely uneconomic, taking into consideration that the compression steel presented in Fig. 2 is already greater than the tension steel at midspan. Several nonlinear FE simulations are carried out with the ratio of midspan compression steel being the only variable. Using $A_s^{'}$ in Fig. 2 as a reference, Figs. 8 to 10 show the tensile damage growth at 50%, 35%, and 30% of $A_s^{'}$. Simulations with lower percentages of $A_s^{'}$

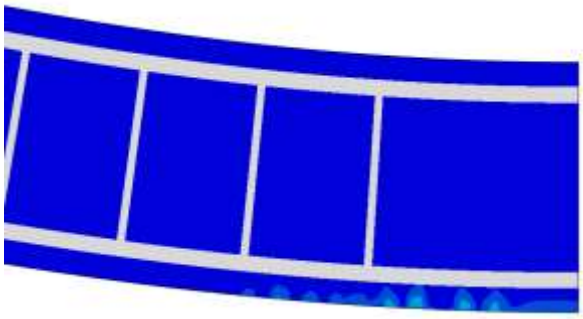

Figure 6. Tensile damage at middle of interior span using $A_s^{'}$

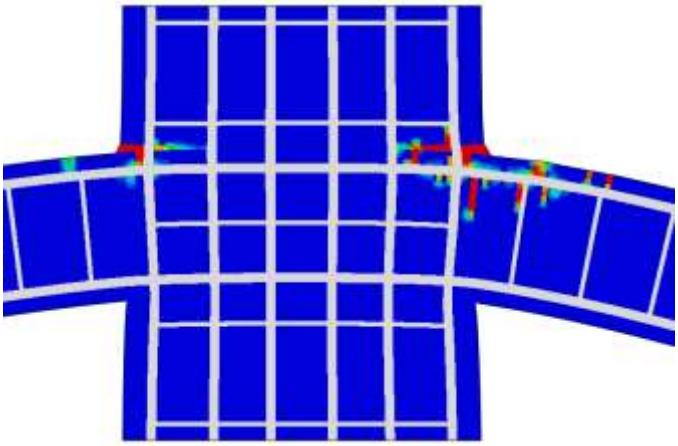

Figure 7. Percentage of compression steel at midspan, 100%

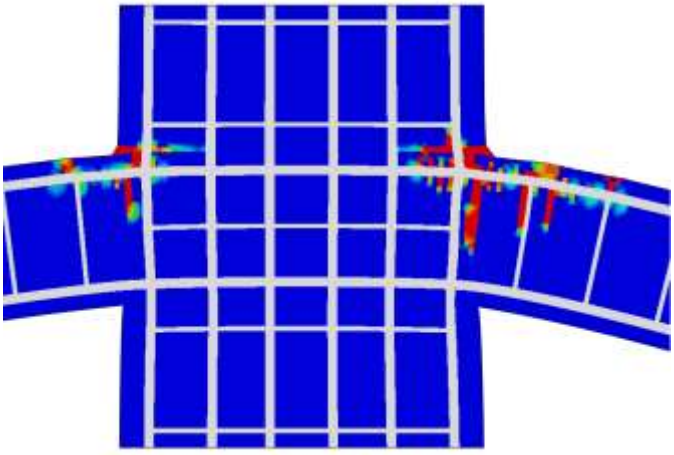

Figure 8. Percentage of compression steel at midspan, 50%

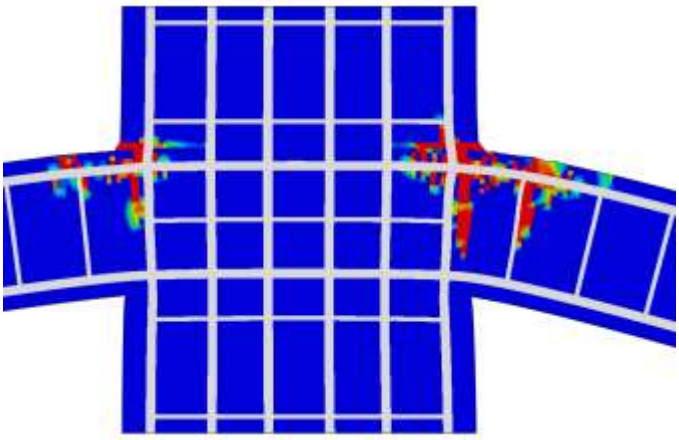

Figure 9. Percentage of compression steel at midspan, 35%

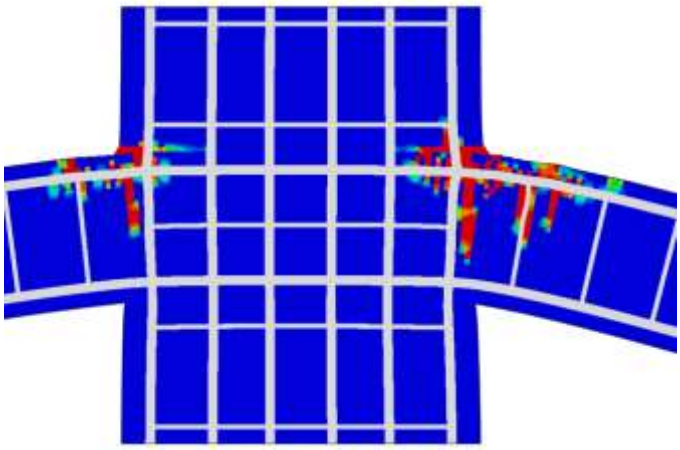

Figure 10. Percentage of compression steel at midspan, 30%

did not converge and their analyses were terminated by ABAQUS.

The deflection at the middle of the interior span is plotted against the applied load for the different value of $A_s^{'}$ just mentioned. The comparison is illustrated in Fig. 11. The decrease of $A_s^{'}$ is accompanied by an increase in midspan deflection, which in turn, increases damage growth at the mispan and support sections. Fig. 12 shows the tensile damage growth at the middle of the interior span at 30% of $A_s^{'}$, which can be compared with the tensile damage growth in Fig. 6. The effect of compression reinforcement on delaying damage in concrete at midspan is shown in Fig. 13, where a comparison between a critically damaged finite element on Fig. 12 and the same element on Fig.6 is carried out.

III. Discussion and Conclusions

The ACI Code deflection check procedure shows that the deflection of the beam under consideration is off limits when considering floors supporting or attached to nonstructural elements that are likely to be damaged by excessive deflections, which is the case in residential buildings. On the other hand, the presented FE simulations reveal huge problems concerning immediate deflections and consequent concrete damage under service loads due to the shallow depth of the wide-hidden beam.

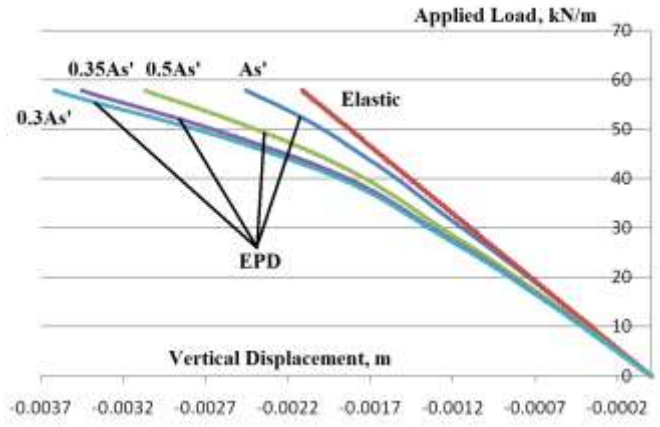

Figure 11. Deflection at middle of the interior span

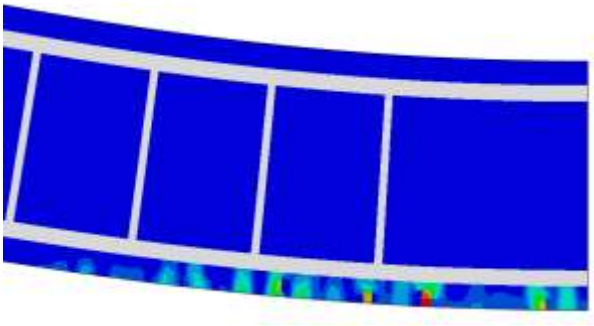

Figure 12. Tensile damage at middle of interior span using 30% of $A_s^{'}$

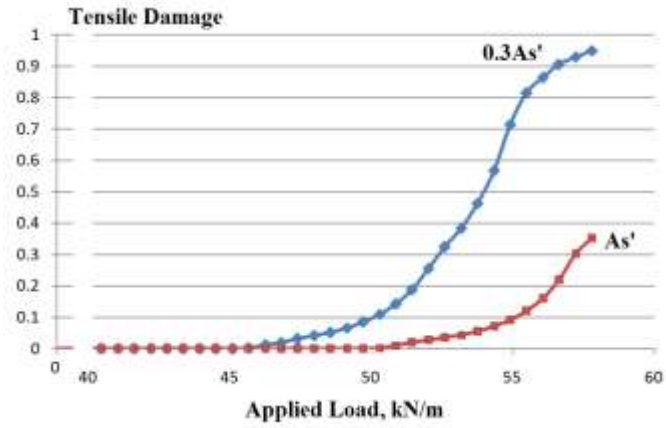

Figure 13. Comparison of Tensile damage at 30% of $A_s^{'}$ and $A_s^{'}$

The effect of compression steel reinforcement on deflection control is clearly noted in the results of the ACI Code procedure as well as the FE simulations. Nevertheless, the effectiveness of it in dragging the deflection values back into the Code's admissible range, or in preventing concrete damage at service loads in the FE simulations, is unimpressive, both physically and economically. The shallow depth of the beam necessitates an amount of compression reinforcement at midspan greater than that required to resist the flexural moments. The misguided procedure of designing the wide-hidden beam for ultimate loads and then "throwing in some" compression reinforcement to control deflection can lead to dreadful consequences. Therefore, the use of such a beam in residential buildings, and where functionality of nonstructural components might be jeopardized, is questionable. Other alternatives, although less aesthetically pleasing, might be more attractive on all other aspects.

References

[1] American Concrete Institute Committee 318. Building Code Requirements for Structural Concrete (ACI 318-11) and Commentary (ACI 318M-11). Farmington Hills, MI, USA, 2011.

[2] ABAQUS User Manual, Version 6.10-1, Dassault Systems Simulia Corporation, Providence, RI, USA, 2010.

[3] Jordanian Code for Loads and Forces, Jordanian National Building Councel, Ministry of Public Works, Jordan, 2nd Edition, 2006.

[4] ACI Committee 435, "Deflection of reinforced concrete flexural members," ACI Journal, Proceedings, vol. 63, no. 6, pp. 637-674, 1966.

[5] J. Lee, and G. L. Fenves, "A plastic-damage model for cyclic loading of concrete structures," J. Eng. Mech., ASCE, vol. 124, no. 8, pp. 892–900, 1998.

[6] Z. N. Taqieddin, G. Z. Voyiadjis, and A. H. Almasri, "Formulation and verification of a concrete model with strong coupling between isotropic damage and elastoplasticity and comparison to a weak coupling model," J. Eng. Mech., ASCE, vol. 138, no. 5, pp. 530-541, 2012.

About Author:

Dr. Taqieddin is an Assistant Professor of Civil Engineering at ASU, Amman, Jordan. BSc 2001 graduate of ASU. MSc 2005 and PhD 2008 graduate of LSU, LA, USA. Research interests include Mechanics of Solids and Structures. Material Modeling and Characterization. Nonlinear Computational Mechanics (Continuum Damage Mechanics and Plasticity).